Carbohydrate Polymer Technologies and Applications 6 (2023) 100380

Contents lists available at ScienceDirect

Carbohydrate Polymer Technologies and Applications

journal homepage: www.sciencedirect.com/journal/carbohydrate-polymer-technologies-and-applications

Supramolecular systems based on chitosan and chemically functionalized nanocelluloses as protective and reinforcing fillers of paper structure

Lorenzo Lisuzzo [a], Giuseppe Cavallaro [a,b,*], Giuseppe Lazzara [a,b], Stefana Milioto [a,b]

[a] Dipartimento di Fisica e Chimica, Università degli Studi di Palermo, Viale delle Scienze, pad. 17, Palermo 90128, Italy
[b] Consorzio Interuniversitario Nazionale per la Scienza e Tecnologia dei Materiali, INSTM, Via G. Giusti, 9, I-, Firenze 50121, Italy

ARTICLE INFO

Keywords:
Nanocellulose
Chitosan
Electrostatic Interactions
ITC
Paper consolidation

ABSTRACT

Supramolecular systems based on chitosan and cellulose nanofibers (CNFs) with a different surface modification (TEMPO-oxidation and carboxymethylation) were investigated and utilized for the functional consolidation of paper. Prior to the paper consolidation, the interactions between chitosan and CNFs dispersed in aqueous solvent were studied. It was detected that the peculiar surface functionalization of nanocellulose is crucial to control the chitosan/CNFs electrostatic attractions and, consequently, the entropic/enthalpic contributions and the stoichiometry of the biopolymer adsorption onto the cellulose nanofibers. Dynamic Light Scattering and rheological experiments revealed that the presence of biopolymeric chains on the CNFs surface favors the entanglement and the aggregation between the nanofibers reinforcing their network. It was observed that chitosan and nanocellulose exhibit synergetic effects on the paper consolidation in terms of reinforcing action, surface hydrophobization and enhancement of the fire-resistance. In conclusion, this paper demonstrates that the electrostatic interactions between chitosan and functionalized nanocellulose drive the formation of hybrid fillers suitable for paper consolidation. Chitosan coated CNFs possess an improved capacity to penetrate the paper structure causing an enhancement of the mechanical resistance and surface hydrophobization. Moreover, chitosan/CNFs create a protective barrier for heat transfer that prevents the paper combustion.

Introduction

In recent years, cellulose nanofibers (CNFs) have attracted a growing interest because of their biocompatibility combined with their unique properties, such as low density, chirality, anisotropic shape, reactive surface chemistry and high stiffness (Ai et al., 2022; Salas et al., 2014). Literature reports that nanocellulose can be employed for numerous biomedical applications including the immobilization of proteins (Bisht et al., 2023; Ong et al., 2023; Tamaddon et al., 2020) and nucleic acids (Pötzinger et al., 2019), the loading and controlled release of drugs (Lisuzzo et al., 2020; Shi et al., 2022) and the fabrication of scaffolds for tissue engineering (Lu et al., 2023; Monfared et al., 2021; Zhang et al., 2020). It is largely demonstrated that CNFs are effective as fire retardants (Charreau et al., 2020; Hu et al., 2021) as well as adsorbent materials for removal of both inorganic and organic contaminants (Barhoum et al., 2023; Faiz Norrrahim et al., 2021; Paul & Ahankari, 2023). Cellulose nanofibers are suitable catalytic supports as reported for the reduction of nitrophenols in water (Gopiraman et al., 2018). Recently, photosynthetic cell factories for biocatalytic ethylene production were obtained by the immobilization of cyanobacteria within hydrogel films based on CNFs and polyvinyl alcohol (Rissanen et al., 2021). As reported in a recent review (Zhao et al., 2020), nanocellulose can be employed as reinforcing filler of polysaccharides to fabricate nanocomposite materials suitable for food packaging applications. The combination of nanocellulose with ionic liquids drives to the production of hybrid membranes useful for gas-separation applications (Janakiram et al., 2020). Within Cultural Heritage, nanocellulose can be employed for the protective coating of textile and paper samples (Spagnuolo et al., 2022).

The properties and the potential applications of cellulose nanofibers depend on their source as well as the production method (Thakur et al., 2021). In general, nanocellulose is obtained from plant-raw materials, such as wood pulp, wheat straw, cotton, and sugar beet, through mechanical defibrillation combined with chemical pre-treatments, which aim to enhance the extraction capacity by the surface functionalization of the cellulosic materials (Thakur et al., 2021). The effective modification of the nanocellulose surface can be achieved by exploiting different chemical reactions that involve efficacious -OH groups of

* Corresponding author.
E-mail address: giuseppe.cavallaro@unipa.it (G. Cavallaro).

https://doi.org/10.1016/j.carpta.2023.100380

Available online 19 October 2023

cellulose. In this regard, TEMPO (2,2,6,6-tetramethylpiperidine-1-oxyl) mediated oxidation, sulfonation, phosphorylation and carboxymethylation represent the main chemical routes to synthesize functionalized cellulose nanofibers (Thakur et al., 2021). As a general consideration, the diameter of cellulose nanofibers range between 3 and 100 nm, while their length is in the order of several micrometers depending on the synthesis procedure (Mokhena & John, 2020).

Chitosan is an emerging biopolymer because of its hydrophobicity as well as its antimicrobial capacity (Cavallaro et al., 2021). Regarding the biomedical applications, chitosan was used to develop drug carriers for cancer therapies (Li et al., 2021) and bone regeneration biomaterials (E. A. Naumenko et al., 2016; E. Naumenko & Fakhrullin, 2019; Zheng et al., 2019). Chitosan/collagen blends filled with clay nanotubes are suitable for hemostatic dressing due to their antimicrobial properties, cytotoxicity and high hemocompatibility (Lin et al., 2023). Hydrogel networks formed by chitosan, collagen and fucoidan can be employed in tissue engineering (Carvalho et al., 2021). Chitosan beads containing metal–organic frameworks (Sadjadi et al., 2023) and Pd nanoparticles (Farrokhi et al., 2022) are efficient and recyclable catalysts. The dispersion of inorganic nanoparticles within the chitosan matrix induced the formation of functional bionancomposites useful for food packaging applications (Bertolino et al., 2016; Cavallaro et al., 2021). Chitosan/halloysite composite films with a sandwich-like morphology exhibited a relevant fire- resistance (Bertolino et al., 2018). As reported in recent articles (Baglioni & Chelazzi, 2021), chitosan is a suitable polymer for numerous applications within the conservation of Cultural Heritage. Chitosan was employed for the preparation of hydrogels with cleaning capacity towards marble surfaces (Cavallaro et al., 2019). Linen textile samples were successfully protected by their consolidation through chitosan coated with Ag-SeO_2 composites (Abdel-Kareem et al., 2015). Calcium/chitosan nanoparticles prepared by ionic gelation method were used for antimicrobial coating of historical paper documents (Egil et al., 2022).

In this work, supramolecular systems based on chitosan and differently functionalized CNFs were investigated to develop functional fillers for paper consolidation. In detail, TEMPO-oxidized CNF (TM-CNF) and carboxymethylated CNF (CM-CNF) were considered because of their high negative charge (Thakur et al., 2021), which can drive to strong interactions with cationic chitosan because of electrostatic attractions. Moreover, both TM-CNF and CM-CNF possess well-defined sizes with large surface area that can be positive for paper consolidation (Thakur et al., 2021). The optimization of the experimental conditions for the paper treatment by immersion method was achieved by a preliminary study on the interactions between chitosan and cellulose nanofibers. Due to the opposite charges of chitosan and nanocelluloses, it is expected that the electrostatic attractions drive to the spontaneous adsorption of the cationic biopolymer onto both TM-CNF and CM-CNFs. Accordingly, the different surface functionalization (TEMPO-oxidation and carboxymethylation) might affect the thermodynamics and stoichiometry of chitosan/nanocelluloses interactions. In relation to the thermodynamic and electrostatic characteristics of chitosan/CNFs interactions, it can be hypothesized that the biopolymer adsorption onto chemically modified cellulose nanofibers could induce synergetic effects on the paper consolidation in terms of improvement of mechanical performances, surface hydrophobization and fire-retardant action. To verify this hypothesis, mechanical properties, wettability and flame-resistance of paper samples treated by CNFs, chitosan and chitosan/CNFs composites were determined.

Materials and methods

Materials

Chitosan extracted from shrimp shell (average molecular weight of 120 kg mol^{-1} and deacetylation degree of 75–85 %) is a Sigma product. Chemically modified cellulose nanofibers (CNFs) were provided by Nippon Paper Industries Co., Ltd., Japan. Specifically, TEMPO-oxidized CNF (TM-CNF) and carboxymethylated CNF (CM-CNF) were investigated. Details on the synthesis, chemical structures and TEM images of both TM-CNF and CM-CNF are reported in Supplementary Material. Based on the technical details provided by Nippon Paper Industries Co. (Lazzara et al., 2018), the width of TM-CNF is 3 nm, while that of CM-CNF ranges between 3 and 15 nm.

Paper (thickness 0.15 mm, 73 g m^{-2} and water capillary raise >178 mmh^{-1}) is from Albet®.

Characterization of chitosan/CNFs aqueous dispersions

Isothermal titration calorimetry (ITC)

The thermodynamics of chitosan/nanocellulose interactions was determined by Isothermal Titration Calorimetry (ITC) experiments, which were performed using an ultrasensitive Nano-iTC200 calorimeter (Micro-Cal). An amount of 40 μL of the chitosan aqueous solution (concentration of 1 g L^{-1}, pH = 4.5) was injected into the thermally equilibrated ITC cell (200 μL) containing the water/nanocellulose dispersion (concentration of 0.01 g L^{-1}, pH = 4.5). Each addition step was 0.49 μL. Volumes were calibrated by NaCl dilution experiment. The cell was thermally equilibrated at 25.000 ± 0.005 °C. The calorimeter sensitivity is at least 2 nanoW. The raw data were corrected for the instrument time constant, and an appropriate baseline was subtracted. As reported elsewhere for chitosan/nanoparticles composites (Bertolino et al., 2017), ITC data were successfully fitted by means of a Langmuir-type adsorption model, which allowed us to estimate the thermodynamic parameters and the stoichiometry for the chitosan/CNFs interactions. Details for the fitting analysis of ITC data are presented in Supplementary Material.

ζ-potential and dynamic light scattering (DLS)

The role of the electrostatic interactions for the chitosan adsorption onto the nanocellulose was investigated by studying the surface charge of biopolymer/CNFs aqueous mixtures at variable composition. To this purpose, ζ-potential experiments were conducted through a Zetasizer Nano-ZS (Malvern Instruments) apparatus. The latter was also used to perform dynamic light scattering (DLS) measurements with the aim to investigate the effects of the chitosan/nanocellulose interactions on the aqueous diffusivity of the nanofibers.

Both DLS and ζ-potential measurements were performed at constant temperature (T = 25 °C). As concerns ζ-potential measurements, a disposable folded capillary cell was used. Regarding DLS tests, the wavelength and the scattering angle were 632.8 nm and 173°, respectively. The field-time autocorrelation functions were analysed by ILT to obtain the distribution of the aqueous diffusion coefficients.

The experiments were performed on chitosan/nanocellulose mixtures in water pH = 4.5. The nanocellulose concentration was kept constant at 0.05 wt%, while the concentration of chitosan was systematically varied to investigate dispersions with a variable biopolymer/CNFs mass ratio (from 0.05 to 3). For comparison, the measurements were performed on aqueous dispersions containing pristine nanocellulose (concentration of 0.05 wt%) as well as pristine chitosan (concentration of 0.05 wt%).

Conductivity measurements

In addition to ζ-potential measurements, the influence of the electrostatic attractions between chitosan and cellulose nanofibers was explored by conductivity titrations, which were performed through a digital Metrohm 660 conductimeter at a frequency of 2 kHz. An amount of 8 mL of the chitosan solution (concentration of 1 g L^{-1}, pH = 4.5) was injected into a cell (25 mL) containing the water/nanocellulose dispersion (concentration of 1 g L^{-1}, pH = 4.5). Each addition step was 0.2 mL. Conductometric measurements were conducted at 25 °C.

Rheological investigations

The effects of the chitosan adsorption on the rheological behavior of cellulose nanofibers were explored using a rheometer (Discovery HR-1, TA Instruments) equipped with a parallel plate (40 mm diameter and 1 mm gap size). Rheological experiments were conducted on chitosan/CNFs mixtures with a mass ratio of 0.1, which represents the stoichiometric composition to achieve the complete saturation of the cellulose nanofibers. Shear-viscosity tests in a flow ramp mode by increasing the shear rate from 0.1 to 1000 s^{-1} within 60 s were carried out. The obtained flow curves (viscosity vs shear rate) were successfully analyzed by using the Cross equation (Cavallaro et al., 2022). In addition, viscoelastic properties were investigated through frequency sweep tests, which were conducted with a constant strain amplitude (1 %) and a variable angular frequency (from 0.01 to 10 Hz). On this basis, we determined the dependence of the storage (*G'*) and loss (*G''*) moduli on the angular frequency.

Paper consolidation by chitosan/CNFs aqueous dispersions

Paper samples were consolidated using the immersion protocol described elsewhere for polymer/nanoclays aqueous dispersions (Cavallaro et al., 2018). Briefly, paper specimens with a rectangular shape (40 mm × 8 mm) were immersed in chitosan/CNFs aqueous dispersions kept on a basculation plan for 24 h at 25 °C. Afterwards, the consolidated paper specimens were dried at 25 °C under vacuum. Chitosan, CNFs and chitosan/CNFs (mass ratio of 0.1) dispersions were employed as consolidant systems. The characteristics of paper and the amounts of consolidants entrapped within its structure are reported in Supplementary Material.

Characterization of paper samples treated by chitosan/CNFs dispersions

Mechanical experiments

The efficiency of the consolidation was evaluated by studying the tensile properties of the treated paper samples. Tensile tests were performed by a DMA Q800 apparatus (TA Instruments) under a controlled stress ramp (1 MPa min^{-1}) at 25.0 ± 0.1 °C.

Water contact angle measurements

The influence of the consolidants on the paper wettability was investigated by water contact angle measurements, which were performed by the sessile drop method using OCA 20 (Data Physics Instruments) equipped with a video measuring system having a high-resolution CCD camera. Interestingly, contact angle data are suitable to highlight hydrophobization effects on the paper surface. The experiments were performed at 25.0 ± 0.1 °C.

Scanning electron microscopy (SEM)

The morphology of paper samples treated by chitosan/TM-CNF and chitosan/CM-CNF were studied by Scanning Electron Microscopy (SEM) using ESEM FEI QUANTA 200F electronic microscope. To avoid charging under the electron beam, each paper sample was coated with Au in argon by means of an Edwards Sputter Coater S150A. The measurements were conducted in high vacuum mode (<6 × 10^{-4} Pa) for simultaneous secondary electrons. Tthe energy of the beam was 25 kV and the working distance was 10 mm.

Flame resistance of consolidated paper

The flame resistance of paper samples (before and after the consolidation) was studied by burning experiments, which were carried out on sheets (20 and 5 mm in length and width, respectively) placed horizontally and ignited at one end. The paper burning was monitored by High-Speed Micro Video Recording system (AOS Technologies - L-VIT 2500) following the combustion front propagating along the media.

Table 1
Interaction parameters for nanocellulose/chitosan obtained from ITC measurements at 25 °C.

Nanocellulose	Z[a] (g_{Chit} g_{CNF}^{-1})	K_{int}[a] (dm^3 mol^{-1})	ΔH_{ads}[a] (kJ mol^{-1})	ΔG_{ads}[b] (kJ mol^{-1})	ΔS_{ads}[c] (kJ mol^{-1} K^{-1})
CM-CNF	0.11 ± 0.03	(1.11 ± 0.06) •10^7	3.22 ± 0.18	−40 ± 2	0.146 ± 0.019
TM-CNF	0.09 ± 0.03	(9.1 ± 0.8) •10^6	2.97 ± 0.13	−39 ± 3	0.143 ± 0.016

[a] from fitting of ITC data
[b] calculated as -ln(K_{int})/RT
[c] calculated as (ΔH_{ads} - ΔG_{ads})/T.

Results and discussion

Thermodynamics of chitosan/CNFs interactions

The thermodynamics of the chitosan adsorption onto both cellulose nanofibers (TM-CNF and CM-CNF) was investigated by ITC experiments using the stepwise injection procedure. It should be noted that the thermal effects of the chitosan/CNFs interactions were estimated by subtracting the effects of dilution of both components (biopolymer and nanocellulose) from the heats of titration. On this basis, the cumulative variation of enthalpy (ΔHic) was determined at variable chitosan/nanocellulose mass ratio (Fig. 2). The obtained trends were successfully fitted by the Langmuir adsorption model for both TM-CNF and CM-CNF. Mathematical details for the fitting model are presented in Supplementary Material.

Based on the ITC data analysis, the enthalpy (ΔH_{ads}) and the equilibrium constant (K_{ads}) were calculated for the biopolymer adsorption onto the cellulose nanofibers. As shown in Table 1, ΔH_{ads} values are positive for both cellulose nanofibers highlighting that the adsorption processes are endothermic. Moreover, it can be stated that the different surface modification of cellulose (TEMPO oxidation and carboxymethylation) slightly affects the affinity of chitosan towards the nanofibers according to the similar K_{ads} values of TM-CNFs and CM-CNFs (Table 1).

The complete description of the energetics of the chitosan adsorption onto the cellulose nanofibers was achieved by the determination of the standard free energy (ΔG_{ads}) and the entropy (ΔS_{ads}), which were calculated according to the classical thermodynamic equations using the K_{ads} and ΔH_{ads} data obtained by the fitting of ITC curves. As a general consideration, ΔG_{ads} is negative highlighting that chitosan spontaneously interacts with the nanocellulose surface, while the positive ΔS_{ads} values indicate that de-hydration and release of counterions are the dominant entropic factors during the adsorption process (Table 1). This finding agrees with the chemical structure of both TM-CNF and CM-CNF, which possess Na^+ counterions that can be released because of the chitosan adsorption. Based on the calculated thermodynamic parameters, it can be concluded that the interactions between cationic chitosan and cellulose nanofibers are spontaneous ($\Delta G_{ads} < 0$), endothermic ($\Delta H_{ads} > 0$) and entropy-driven ($\Delta S_{ads} > 0$). Accordingly, literature reports that the adsorption of ionic molecules onto the nanocellulose surface are mostly endothermic and favored by entropic contributions due to the release of surface-structured water molecules and counterions from the electric double layer caused by the interaction between opposite charges (Lombardo & Thielemans, 2019). The influence of the electrostatic interactions on the thermodynamics of chitosan/CNFs interactions will be discussed in the following paragraph by considering additional data, including ζ-potential results and conductivity titrations. It should be noted that the chitosan adsorption onto the CNFs surface generates another microscopic mechanism (the reduction of the configuration freedom of the biopolymeric chains), which induces a decrease of entropy. Based on the ITC results (Table 1), it can be stated that the entropic effect of this process is lower with respect to the release

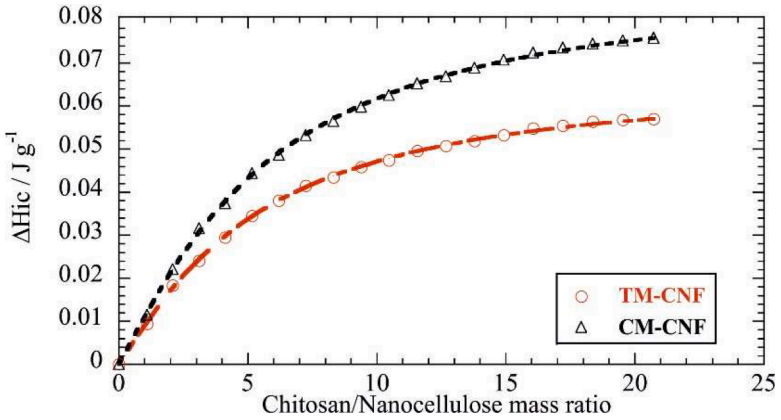

Fig. 1. Cumulative enthalpy variation data obtained by isothermal titration of both cellulose nanofibers (TM-CNF and CM-CNF) with chitosan. Lines correspond to the best fits according to the Langmuir adsorption model.

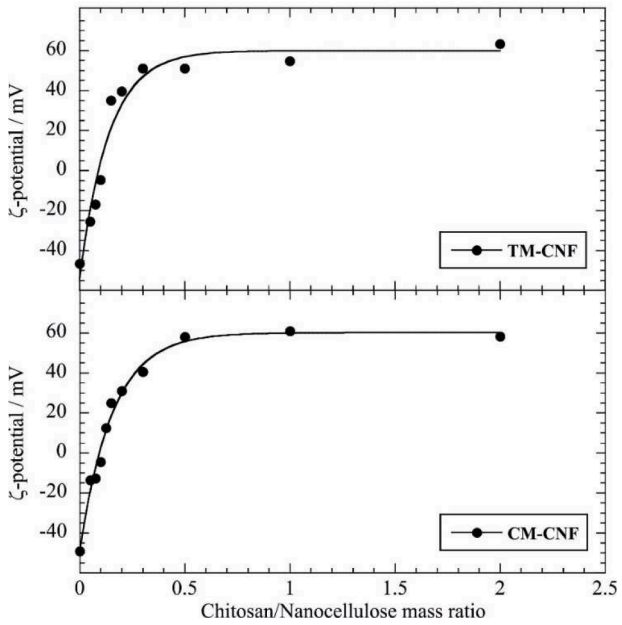

Fig. 2. Dependence of the ζ-potential on the chitosan/nanocellulose mass ratio for both cellulose nanofibers (TM-CNF and CM-CNF). Lines correspond to the fitting according to an exponential rise equation.

of Na^+ ions and water molecules at the chitosan/nanocellulose interface. Similar results were detected for the adsorption of polymer onto laponite nanodisks, which possess Na^+ ions on their surface (Cavallaro et al., 2012). Besides the thermodynamic parameters, the fitting of the ITC curves (Fig. 1) allowed us to determine the chitosan/nanocellulose stoichiometric ratio (Z) at the saturation point. Namely, Z values represent the maximum adsorption amounts of chitosan per gram of cellulose nanofibers (TM-CNF and CM-CNF). The chitosan/CNFs stoichiometry was slightly larger for CM-CNF compared to that of TM-CNF. On this basis, it can be asserted that carboxymethylation induces the formation of cellulose nanofibers able to adsorb a larger amount of polymer on their surface with respect to nanocellulose functionalized by TEMPO oxidation.

Electrostatic aspects of chitosan/CNFs interactions

ITC results revealed that the chitosan adsorption onto the nanocellulose surfaces depends on the electrostatic characteristics of the biopolymer and the nanofibers. Namely, it can be stated that the interactions between chitosan and cellulose nanofibers are strongly affected by the electrostatic attractions between chitosan and nanocellulose, which possess opposite surface charges under the investigated acidic conditions (pH = 4.5) of the aqueous medium. A deeper description on the relation between chitosan/nanocellulose interactions and the corresponding surface charges of both components was achieved by measuring the ζ-potential of aqueous mixtures at variable composition. Fig. 2 shows the dependence of the ζ-potential on the chitosan/nanocellulose mass ratio for both TM-CNF and CM-CNF.

It should be noted that ζ-potential data at mass ratio equals to 0 represent the surface charge of pristine cellulose nanofibers. According to their surface chemistry, both nanocelluloses are negatively charged as demonstrated by their ζ-potential (-46.6 ± 1.4 mV and -49.2 ± 1.5 mV for TM-CNF and CM-CNF, respectively). Oppositely, pure chitosan presents a positive charge in agreement with its ζ-potential ($+60.1 \pm 1.8$ mV). These results confirm that the interactions between chitosan and both nanocelluloses are mostly controlled by their electrostatic attractions as hypothesized by the calculated thermodynamic parameters, which revealed that the biopolymer adsorption onto the nanofibers is entropy-driven ($\Delta S_{ads} > 0$). This consideration is supported by comparing the ζ-potential data of pristine cellulose nanofibers, which highlighted that content of negative charges on the surface of CM-CNFs is higher respect to that on the surface of TM-CNF. Namely, the surface density of CH_2COO^- groups on CM-CNF is larger than that of COO^- groups on TM-CNF in agreement with the technical details provided from Nippon Paper Industries Co. (Lazzara et al., 2018) Therefore, the amount of Na^+ counterions on the surface of CM-CNF is superior compared to that on TM-CNF. Consequently, it can be expected that the entropic contribution due to the Na^+ ions release is higher for the chitosan adsorption onto the carboxymethylated nanocellulose. This hypothesis agrees with ΔS_{ads} results obtained by the fitting of ITC curves (Table 1). As a general result, the dependence of the ζ-potential on the chitosan/nanocellulose mass ratio showed a monotonic increasing trend reaching the value of pristine chitosan. In particular, both trends can be divided in two regions: 1) ζ-potential < 0 and 2) ζ-potential > 0. In the first region, the addition of chitosan generated a decrease of the ζ-potential absolute value that could be attributed to the partial neutralization of the negative surface charges of the cellulose nanofibers because of the biopolymer adsorption. The negative ζ-potential values of the first region evidence that nanocellulose surface was not saturated by chitosan. It is important to note that the ζ-potential becomes null once the saturation point is achieved and, consequently, the adsorbed chitosan completely neutralizes the negative surface charges of the cellulose nanofibers. On the other hand, the second region shows positive ζ-potential values highlighting that the aqueous dispersion contains an excess of chitosan respect to the saturation point. Therefore, a fraction of the biopolymeric chains (positively charged) are freely dispersed in

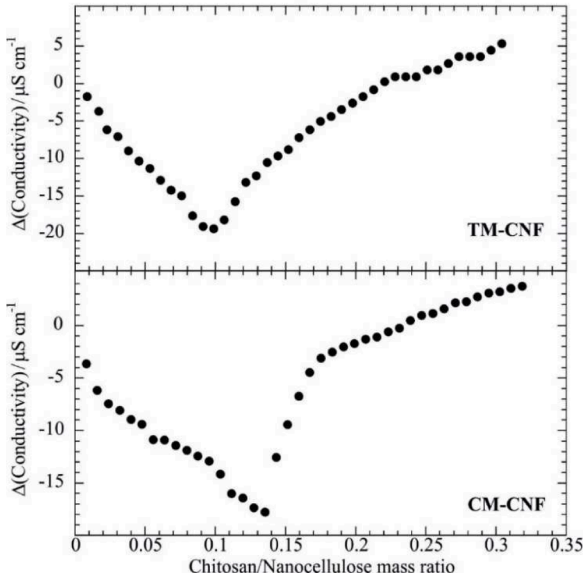

Fig. 3. Conductivity titration curves for chitosan/TM-CNF and chitosan/CM-CNF mixtures. The conductivity data are presented as absolute variations with respect to the conductivity values of pristine nanocelluloses in water.

water explaining the positive ζ-potential data. It should be noted that the ζ-potential values are close to that of pristine biopolymer for high chitosan/nanocellulose mass ratios (ca. 2 order of magnitude higher than the stoichiometry) because the content of unbound chitosan is largely predominant.

Furthermore, the analysis of the ζ-potential data allowed us to estimate the chitosan/nanocellulose stoichiometric ratios, which were compared to those determined by ITC measurements. To this purpose, the experimental curves of ζ-potential vs chitosan/nanocellulose mass ratio were fitted using an exponential rise equation for both TM-CNFs and CM-CNFs. Based on the obtained fitting functions, the ratios corresponding to the null ζ-potential values were calculated. The saturation point of the nanofibers was achieved for chitosan/nanocellulose mass ratios equal to 0.10 ± 0.02 and 0.12 ± 0.02 for TM-CNFs and CM-CNFs, respectively. These results are in good agreement with those determined from the thermodynamic investigations.

In addition to the ζ-potential measurements, the electrostatic aspects of the chitosan/nanocellulose interactions were explored by studying the effect of the chitosan adsorption on the conductivity of the cellulose nanofibers dispersed in aqueous solvent. Fig. 3 shows the conductivity titration curves for both chitosan/TM-CNF and chitosan/CM-CNF. The conductivity results of the chitosan/nanocellulose mixtures are presented as absolute variations compared to those of pristine cellulose nanofibers. Both titration curves are characterized by an initial decreasing trend that can be attributed to the neutralization of the negative charges of the nanocellulose surfaces because of the adsorption of the cationic biopolymer. Then, the conductivity reached a minimum that reflects the complete saturation of the nanocellulose surfaces. According to the calorimetric and ζ-potential experiments, the saturation point was achieved at a larger chitosan/nanocellulose mass ratio for CM-CNF (0.14) with respect to that determined for CM-CNF (0.10). The further addition of chitosan generated an increase of the conductivity because the added biopolymer (positively charged) is not adsorbed on nanocellulose remaining freely dispersed in water.

The combination of the electrostatic and thermodynamic aspects of the chitosan/nanocelluloses interactions allowed us to obtain a comprehensive description of the adsorption of the cationic biopolymer onto chemically modified cellulose nanofibers. Fig. 4 displays a schematic representation of the biopolymer adsorption onto the surfaces of CNFs evidencing that the interactions between chitosan and nanocellulose are influenced by the peculiar functionalization (TEMPO oxidation or carboxymethylation) of the nanofibers.

Effects of the chitosan adsorption on the aqueous dynamics of cellulose nanofibers

The influence of the chitosan adsorption on the dynamics of cellulose nanofibers dispersed in water was investigated. To this purpose, DLS experiments were conducted on aqueous dispersions with variable chitosan/nanocellulose ratio. As a general consideration, the obtained autocorrelation curves were successfully fitted using a monoexponential decay function. Accordingly, the intensity-weighted distributions are unimodal for both pristine cellulose nanofibers and chitosan/nanocellulose mixtures with different composition (Fig. 5 and Supplementary Material). It was observed that the addition of chitosan on both TM-CNF and CM-CNF shifts the distributions to smaller diffusion coefficients highlighting that the aqueous mobility of the cellulose nanofibers is reduced. This effect is enhanced by increasing the chitosan content in the dispersion.

The influence of the chitosan/nanocellulose mass ratio on the aqueous dynamics of cellulose nanofibers is presented in Fig. 6, which

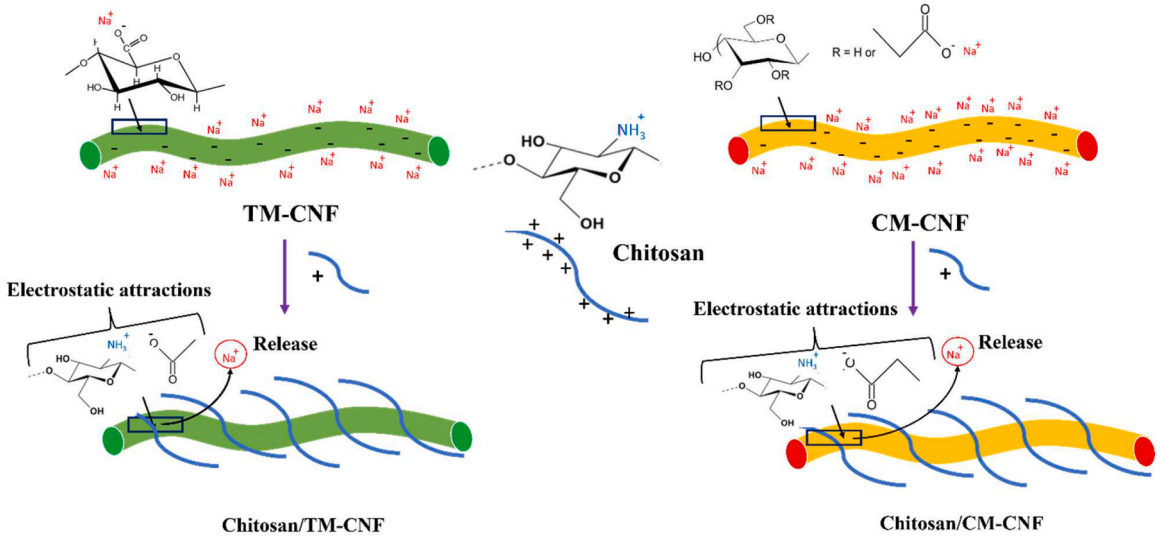

Fig. 4. Schematic representation of the chitosan adsorption onto chemically modified nanocelluloses (TM-CNF and CM-CNF).

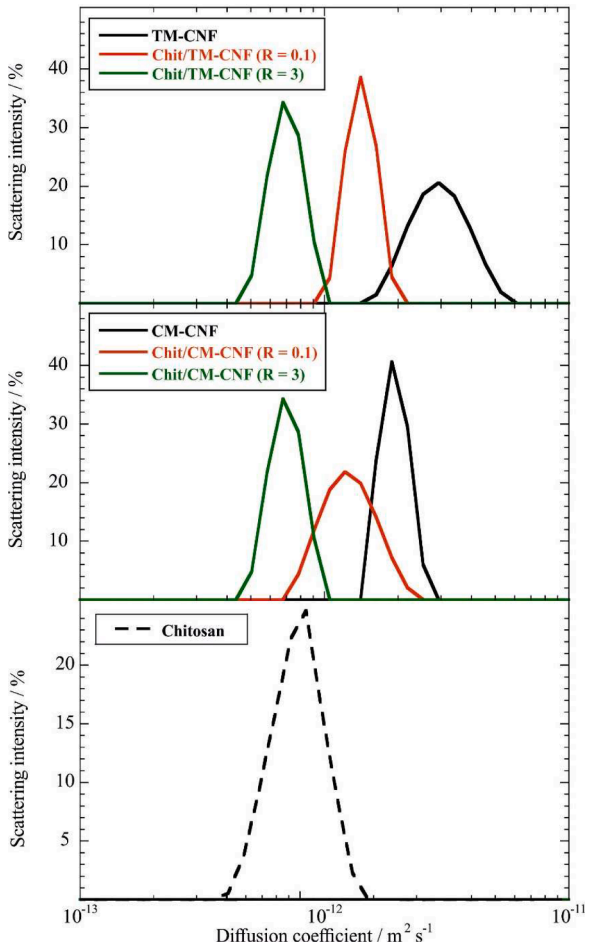

Fig. 5. Intensity-weighted distributions obtained from DLS measurements for the aqueous diffusion coefficient of chitosan, pristine cellulose nanofibers (TM-CNF and CM-CNF) and chitosan/nanocellulose composites at variable mass ratio (0.1 and 3).

reports the average values of the diffusion coefficient obtained from the mathematical analysis of the intensity-weighted distributions.

The enhancement of the chitosan amount induced a decrease of the diffusion coefficient that can be attributed to the polymer adsorption onto CNFs combined with depletion processes. Specifically, the reduction of the aqueous diffusivity of the nanofibers can be ascribed entirely to the biopolymer adsorption for chitosan/nanocellulose ratios equal to ca. 0.1, which represent the saturation point as evidenced by the thermodynamic and electrostatic investigations. Specifically, the chitosan adsorption slows down the dynamics of both TM-CNF and CM-CNF because of attractive hydrophobic interactions between the adsorbed polymeric chains. In addition to the biopolymer adsorption, depletion processes can contribute to the reduction of the CNFs mobility for chitosan/nanocellulose ratio > ca. 0.1 because of the presence of free non-adsorbing polymeric chains in the aqueous medium. Namely, free chitosan can favor the aggregation of the cellulose nanofibers causing an increase of their aqueous diffusion coefficient. This consideration is supported by literature on biopolymer/nanoparticle colloidal systems (Durand-Gasselin et al., 2014).

Influence of chitosan adsorption on the rheological properties of cellulose nanofibers

The influence of the chitosan adsorption on the rheological behavior of the cellulose nanofibers was studied by both shear flow and frequency sweep experiments. Based on the thermodynamic and electrostatic results, the rheological measurements were conducted on chitosan/nanocellulose aqueous mixtures with mass ratio of 0.1, which is close to the stoichiometric ratio for both TM-CNF and CM-CNF. In particular, the concentrations of nanocellulose and chitosan were kept constant at 0.05 and 0.5 wt%, respectively. For comparison, rheological experiments were carried out on 0.5 wt% CNFs aqueous dispersions. The determination of the rheological properties was useful to evaluate the suitability of chitosan/nanocellulose mixtures in water for the paper treatment by immersion protocol.

The flow experiments allowed us to obtain the dependence of the viscosity (η) on the shear rate (γ) for all the investigated dispersions. As displayed in Fig. 7, the η vs γ functions show decreasing trends for both CNFs and chitosan/CNFs highlighting the Non-Newtonian behavior of all the colloids. Similar observations were detected for aqueous dispersions containing TEMPO oxidized nanofibers. The shear-thinning behavior was attributed to the destruction of the nanofibers network at high shear rate inducing a decrease of the measured viscosity (Vadodaria et al., 2018).

As reported for carboxylated cellulose nanofibers synthesized by TEMPO-periodate oxidation (Qu et al., 2021), the flow curves were successfully fitted using the Cross model allowing us to estimate the zero-shear viscosity (η_0), the relaxation time (α) and the shear thinning index (m), which is a dimensionless parameter ranging between 0 (Newtonian fluid) and 1 (plastic fluid). The fitting parameters obtained by the analysis of the flow curves with the Cross equation are collected in Supplementary Material.

As concerns the η_0 values, the chitosan addition generated an increase for both TM-CNF and CM-CNF. These results evidence that the chitosan adsorption enhanced the entanglement and the aggregation between CNFs reinforcing their network with a consequent increment of the viscosity. The reinforcing action of the biopolymer on the

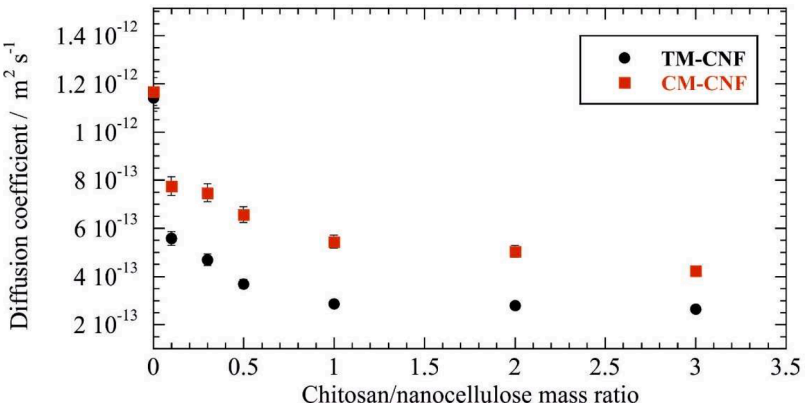

Fig. 6. Aqueous diffusion coefficients of cellulose nanofibers as functions of the chitosan/nanocellulose mass ratio.

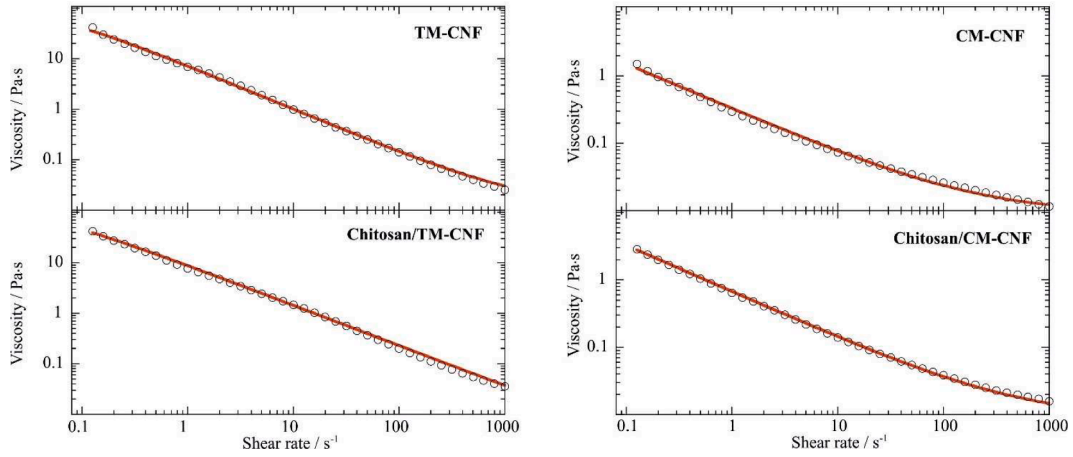

Fig. 7. Flow curves (shear viscosity as a function of shear rate) for cellulose nanofibers (TM-CNF and CM-CNF) and chitosan/cellulose nanofibers mixtures. The concentration of CNFs and chitosan were fixed at 0.5 and 0.05 wt%, respectively.

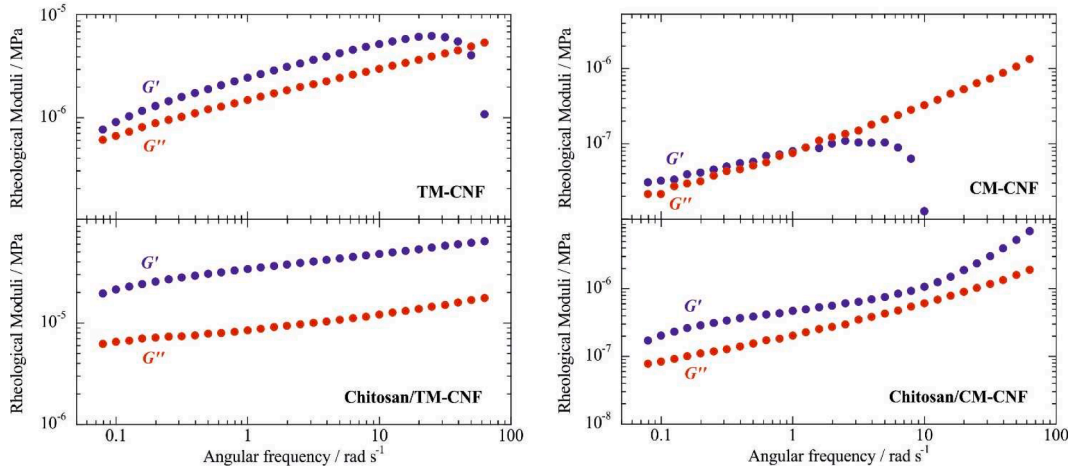

Fig. 8. Storage (*G'*) and loss (*G''*) moduli as functions of the angular frequency for cellulose nanofibers (TM-CNF and CM-CNF) and chitosan/cellulose nanofibers mixtures. The concentration of CNFs and chitosan were fixed at 0.5 and 0.05 wt%, respectively.

nanofibers-based network is stronger for CM-CNF, which evidenced a η_0 enhancement of ca. 2 times due to the interactions between chitosan and nanocellulose. We detected that the different surface functionalization (TEMPO oxidation and carboxymethylation) strongly affects the relaxation time being that the α value of CM-CNF is 4 order of magnitude larger than that of TM-CNF. The chitosan adsorption determined an increase of the relaxation time for both nanocelluloses that reflects the reduction of the aqueous mobility of the cellulose nanofibers. This finding agrees with the DLS data presented in the previous paragraph. As a general result, the calculated m values are lower than 1 confirming that CNFs and chitosan/CNFs aqueous dispersions behave like non-Newtonian pseudoplastic fluids. The results on CNFs aqueous dispersions evidenced that the TEMPO-oxidized nanocellulose possesses a higher pseudoplasticity compared to the carboxymethylated cellulose nanofibers. The chitosan adsorption onto the TM-CNF determined a slight m decrease, which is consistent with a reduction of the shear thinning behavior of the cellulose nanofibers. Oppositely, the presence of chitosan did not alter the pseudoplasticity of carboxymethylated nanocellulose as demonstrated by the similar m values of CM-CNF and chitosan/CM-CNF dispersions.

The influence of the chitosan adsorption on the entanglement and aggregation between the cellulose nanofibers was explored also by frequency sweep experiments, which allowed us to determine the storage (*G'*) and loss (*G''*) moduli of the dispersions under variable angular frequency (ω) (Fig. 8).

As concerns pristine CNFs, it was detected that *G'* and *G''* trends present a crossing point at angular frequency of 45.78 and 1.114 rad s^{-1} for TM-CNF and CM-CNF, respectively. The crossover between *G''* and *G'* represents the sol/gel transition as reported for nanocellulose and biopolymer colloids (Cavallaro et al., 2022; Wu et al., 2021). Before the crossing point, the aqueous dispersions based on pristine nanocelluloses exhibited a gel-like behavior being that *G'* is larger than *G''*. This result could indicate that the long-range rearrangements of the nanofibers are slow. Oppositely, the CNFs dispersions showed a fluid-like behavior (*G''* > *G'*) after the crossing point evidencing that short-range rearrangements are fast. Interestingly, the addition of chitosan changed the dependences of the rheological moduli on the angular frequency. Specifically, it was observed that *G'* is higher than *G''* within the whole frequency range for both chitosan/TM-CNF and chitosan/CM-CNF mixtures. Accordingly, it can be stated that the chitosan/nanocellulose aqueous dispersions behave like a gel for all the investigated frequencies. This finding could indicate that the chitosan adsorption favors the entanglement and aggregation between the nanofibers, which produce more robust networks compared to those based on pristine TM-CNF and CM-CNF. The enhancement of the network strength could be explained by considering the presence of hydrophobic interactions between the cellulose nanofibers coated by the cationic chitosan. These attractions are predominant with respect to the electrostatic interactions

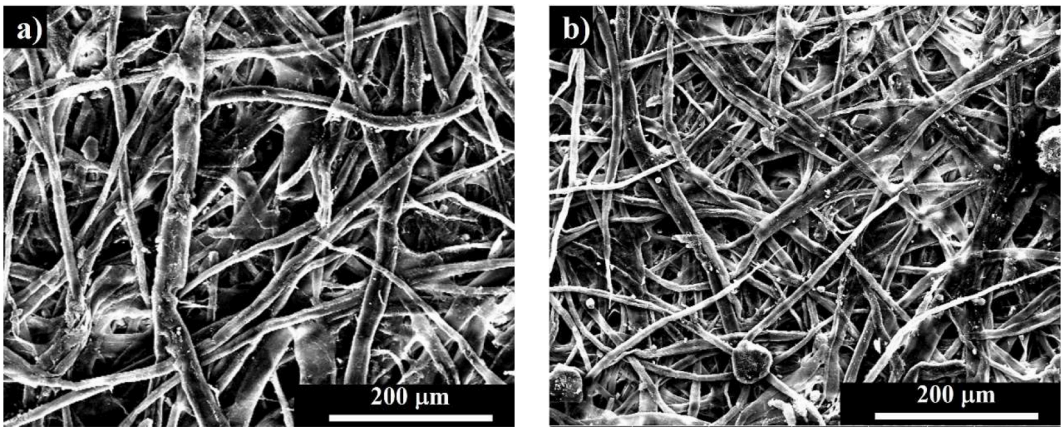

Fig. 9. SEM micrographs of paper samples treated by chitosan/TM-CNF (a) and chitosan/CM-CNF (b) mixtures in water.

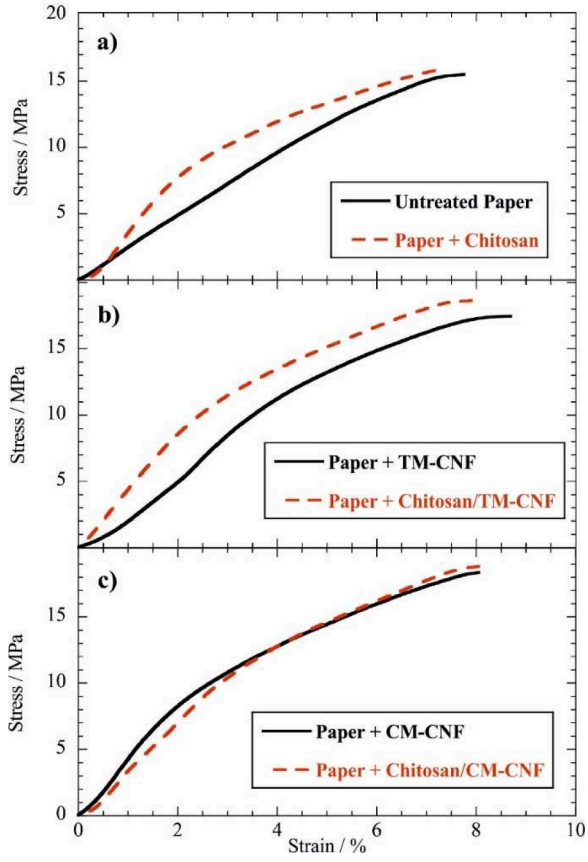

Fig. 10. Stress vs strain curves for paper before and after the treatment by chitosan (a), paper treated by CNF-TM and chitosan/TM-CNF dispersions (b) and paper treated by CNF-CM and chitosan/CM-CNF dispersions (c). The concentration of chitosan was fixed at 0.05 wt%, while that of cellulose nanofibers was kept at 0.5 wt%.

inducing the formation of more robust networks. This hypothesis is supported by the thermodynamic and electrostatic description of the interactions occurring between cellulose nanofibers and chitosan.

Tensile performances, wettability and flame resistance of paper consolidated by chitosan/CNFs mixtures

The chitosan/nanocellulose aqueous mixtures were tested for the paper consolidation by using the immersion protocol presented in the Experimental section. Specifically, the concentrations of CNFs and chitosan (0.5 and 0.05 wt%, respectively) were equivalent to those investigated in the rheological experiments. The morphologies of the paper samples treated by chitosan/TM-CNF and chitosan/CM-CNF mixtures are shown by SEM images (Fig. 9).

For comparison, the paper treatment was conducted with aqueous dispersions of neat CNFs (concentration of 0.5 wt%) as well as pristine chitosan (concentration of 0.05 wt%). It is important to evidence that recent works report that both components are effective as consolidants of paper (Abdel-Kareem et al., 2015; Spagnuolo et al., 2022). Cellulose nanofibers can be employed as reinforcing fillers of the paper structure generating an improvement of the mechanical resistance.(Spagnuolo et al., 2022) As evidenced by a recent review, the paper consolidation efficiency depends on the chemical functionalization of cellulose nanofibers (Spagnuolo et al., 2022). On the other hand, chitosan can be used as flame retardant (Chen et al., 2020; Fang et al., 2022; Kundu et al., 2022) and hydrophobic agent (Martins et al., 2023) enhancing the properties and functionalities of the paper samples. According to these considerations, the tensile performances, wettability and the flame resistance of paper consolidated with chitosan/nanocellulose mixtures were determined to explore possible synergetic effects of the biopolymer and cellulose nanofibers. The tensile properties of untreated and treated paper specimens were studied by Dynamic Mechanical Analysis under a controlled stress ramp. The analysis of the stress vs strain curves (Fig. 10) allowed to determine the tensile parameters of paper in terms of elastic modulus, stress at break and ultimate elongation. The obtained data are collected in Table 3.

It was observed that the addition of chitosan in the consolidating dispersions enhances the capacity of cellulose nanofibers to improve the stress at breaking point of the paper. In particular, the consolidation with pristine TM-CNF and CM-CNF generated improvements by 12 % and 18 %, respectively, while the stress at break of paper consolidated with chitosan/TM-CNF and chitosan/CM-CNF was enhanced by 20 % and 22 %, respectively. These results could indicate that the adsorption of chitosan favors the filling ability of the cellulose nanofibers within the fibrous structure of the paper. Namely, it can be hypothesized that presence of nanocelluloses improved the connection between the fibers in the matrix of the paper driving to an enhancement of the mechanical resistance. Similar results were detected for paper treated by sulfated and neutral cellulose nanocrystals, which favor the interconnection of the paper fibers through the establishment of polar interactions (Operamolla et al., 2021). Literature reports that the filling of historical paper by cellulose nanocrystals improved the tensile strength by ca. 21%. This improvement was enhanced to 27% by using composites based on cellulose nanocrystals and halloysite clay nanotubes as fillers for paper consolidation (Elmetwaly et al., 2022). Halloysite clay nanotubes with hydroxypropylcellulose were employed as nanofillers of paper structure

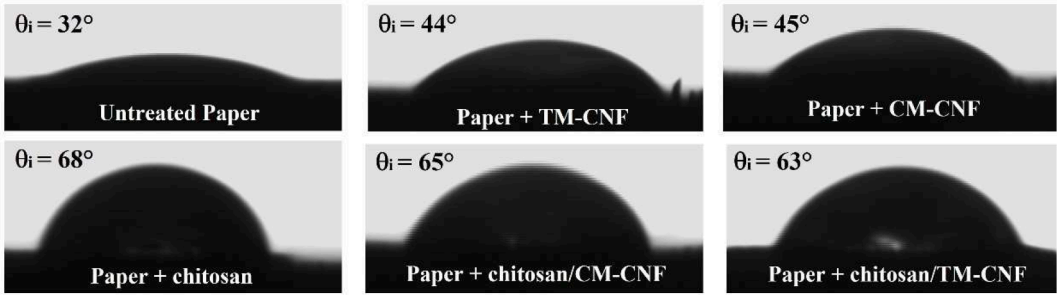

Fig. 11. Images of the water droplets immediately after their deposition on the surface of untreated and treated paper samples. The corresponding contact angle values are presented.

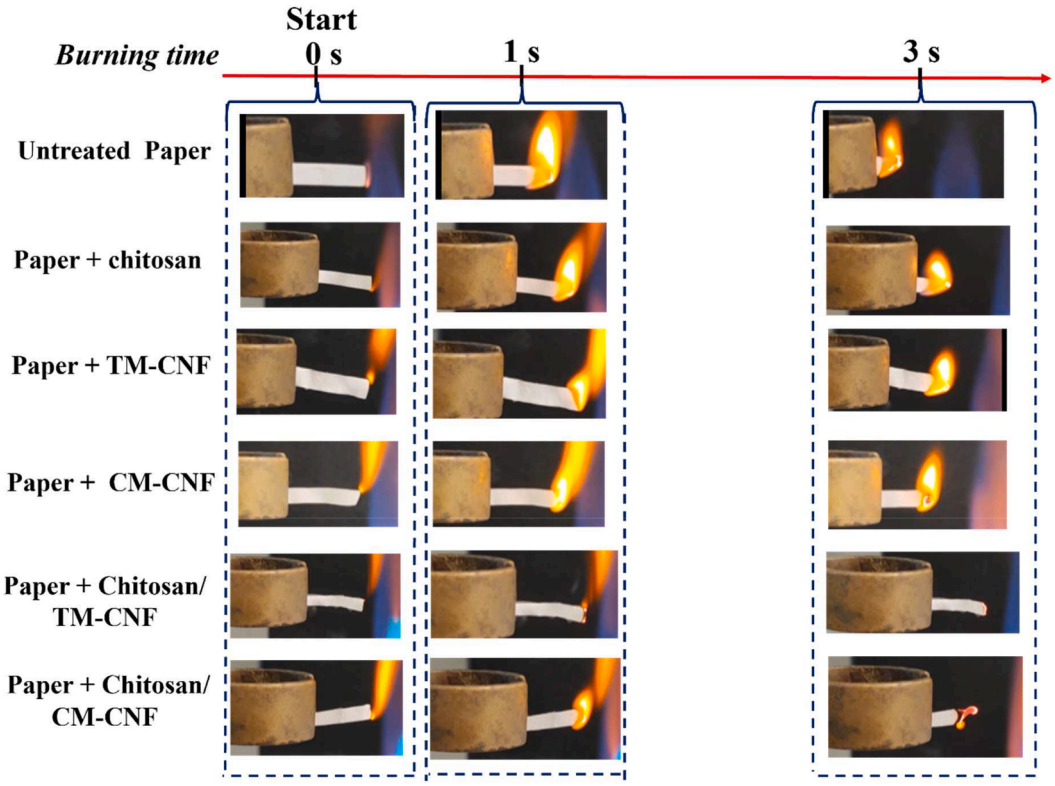

Fig. 12. Images of untreated and treated paper samples during the burning experiments.

inducing an increase of the tensile strength by ca. 10 % (Lisuzzo et al., 2021).

As a general result, the consolidation with both CNFs dispersions and chitosan/CNFs mixtures induced slight increases of the elastic modulus and the ultimate elongation compared to the untreated paper. It should be noted that the treatment by chitosan dispersion did not alter the stress at break of the paper evidencing that the mechanical resistance was not improved by the presence of the pristine biopolymer. On the other hand, the paper treated with chitosan exhibited the highest rigidity as demonstrated by the largest elastic modulus.

The influence of the consolidating systems on the paper wettability was studied by water contact angle experiments. Fig. 11 displays the images of the water droplets (with the corresponding contact angle values θ_i) obtained immediately after their deposition on the surface of the paper samples.

It was detected that the untreated paper presents the lowest θ_i (32°), which is consistent with its hydrophilic nature as reported elsewhere (Cavallaro et al., 2016). The consolidation with pristine nanocelluloses induced a slight hydrophobization of the paper surface as evidenced by the larger θ_i values (44° and 45° for TM-CNF and CM-CNF, respectively). Further increases of the initial contact angle were achieved by using chitosan/CNFs mixtures as consolidating systems highlighting that the presence of biopolymer improved the hydrophobization effect on the paper surface. It should be noted that the paper treated with pristine chitosan presents a contact angle (68°) similar to those determined after the consolidation with chitosan/TM-CNF (63°) and chitosan/CM-CNF (65°). On this basis, it can be stated that the paper hydrohobization generated by chitosan/nanocellulose mixtures can be largely attributed to the biopolymer. In addition, the wettability results highlighted that chitosan could act as hydrophobic agent of paper despite its interactions with CNFs.

Burning experiments on paper samples consolidated with chitosan, CNFs and chitosan/CNFs dispersions were carried out to evaluate the influence of the consolidants as flame retardants. To this purpose, the kinetic evolution of the combustion front of the paper specimens with a rectangular shape was studied. The flame propagation videos are reported in Supplementary Material, while Fig. 12 displays the images of the untreated and treated samples at variable times from the starting

point of the paper burning.

It was observed that the treatment by using the pristine consolidants (chitosan or CNFs) delays the spread of fire after the paper ignition. The analysis of the videos provided the burning rates for paper before and after the consolidation with chitosan, TM-CNFs and CM-CNFs (Table 3). Similar results were detected by using halloysite nanotubes loaded with perfluorooctanoate as fillers of paper (Cavallaro et al., 2016).

Interestingly, the fire spreading was prevented in the paper samples treated with chitosan/TM-CNFs and chitosan/CM-CNFs. Therefore, it can be hypothesized that the chitosan coated nanocelluloses create an efficient protective layer, which stops the heat and mass transfer in the paper combustion. Namely, the chitosan/CNFs hybrids exhibited a stronger fire-retardant action compared to that of the pristine components. This finding could be related to the improved filling capacity within the paper structure of CNFs after the adsorption of chitosan on their surfaces.

Conclusions

An advanced and sustainable protocol for the paper treatment by using aqueous mixtures of chitosan and chemically modified cellulose nanofibers (CNFs) was proposed. The optimization of the paper consolidation was achieved based on the preliminary investigations of the chitosan/nanocellulose supramolecular systems. Among functionalized nanocelluloses, TEMPO-oxidized (TM-CNF) and carboxymethylated (CM-CNF) cellulose nanofibers were selected. Isothermal Titration Calorimetry results evidenced that the chitosan adsorption onto both TM-CNF and CM-CNF is endothermic ($\Delta H_{ads} > 0$) and spontaneous ($\Delta G_{ads} < 0$) in agreement with the opposite charges of chitosan and nanocelluloses. The peculiar CNFs surface functionalization slightly affected the stoichiometry of chitosan/nanocellulose complex. On the other hand, it was observed that the entropic contribution of the biopolymer adsorption is larger for carboxymethylated cellulose nanofibers due to their stronger electrostatic attractions with chitosan, which induces the release of Na^+ counterions from the CNFs surface. This finding agrees with the ζ-potential data highlighting that the surface density of CH_2COO^- groups on CM-CNF is larger than that of COO^- groups on TM-CNF. As evidenced by Dynamic Light Scattering experiments, the chitosan adsorption reduces the aqueous mobility of the cellulose nanofibers, while rheological investigations revealed that the presence of biopolymeric chains on the CNFs surface favors the entanglement and the aggregation between the nanofibers reinforcing their network. According to the obtained results, aqueous mixtures of chitosan (0.05 wt%) and nanocellulose (0.5 wt%) were used for the paper consolidation by the immersion method. The selected concentrations assured that the surface of the cellulose nanofibers is completely saturated by chitosan. The adsorption of chitosan on the CNFs surface revealed an efficient strategy to obtain nanofillers with multiple functionalities towards the treated paper. Specifically, the chitosan adsorption enhanced the reinforcing action of both nanocelluloses towards paper samples as evidenced by the increases of the stress at breaking point values. Moreover, it was observed that the paper treatment by chitosan/CNFs dispersions generates a relevant surface hydrophobization, which does not occur for paper consolidated with pristine nanocelluloses. Interestingly, the consolidation by both chitosan/TM-CNFs and chitosan/CM-CNFs prevents paper combustion. This effect could indicate that the nanofibers coated by chitosan create a protective barrier for the heat transfer during the paper burning. In contrast, the filling of paper with pure consolidants (chitosan or CNFs) induced increases of the burning rate highlighting their slighter fire-retardant action compared to chitosan/CNFs composites. In conclusion, this work demonstrates that supramolecular systems based on chitosan and chemically modified cellulose nanofibers are perspective fillers for the protective consolidation and surface hydrophobization of paper.

Table 2.

Table 2
Tensile parameters of paper samples before and after the treatment by chitosan/CNF mixtures.

Sample	Elastic Modulus[a] (MPa)	Stress at break[a] (MPa)	Ultimate elongation[a] (%)
Untreated Paper	255 ± 26	15.5 ± 1.5	7.75 ± 0.09
Paper + chitosan	502 ± 41	15.9 ± 1.7	7.38 ± 0.08
Paper + TM-CNF	284 ± 29	17.5 ± 1.8	8.69 ± 0.09
Paper + chitosan/TM/CNF	460 ± 40	18.6 ± 1.9	7.96 ± 0.07
Paper + CM-CNF	490 ± 45	18.3 ± 1.5	8.06 ± 0.08
Paper + chitosan/CMCNF	423 ± 40	18.8 ± 1.6	8.19 ± 0.08

[a] calculated from the analysis of stress vs strain curves.

Table 3
Burning rate of untreated and treated paper samples.

Sample	Burning rate / mm s^{-1}
Untreated Paper	5.41
Paper + chitosan	4.63
Paper + TM-CNF	4.04
Paper + CM/CNF	3.82
Paper + chitosan/TM-CNF	n.d.
Paper + chitosan/CMCNF	n.d.

Declaration of Competing Interest

The authors declare that they have no known competing financial interests or personal relationships that could have appeared to influence the work reported in this paper.

Data availability

Data will be made available on request.

Acknowledgments

The work was financially supported by FFR 2023 and University of Palermo.

This work was funded by the European Union (NetGeneration EU) through the MUR-PNRR project SAMOTHRACE (ECS00000022).

"TM-CNF" and "CM-CNF" samples were kindly provided by Nippon Paper Industries Co.

Supplementary materials

Supplementary material associated with this article can be found, in the online version, at doi:10.1016/j.carpta.2023.100380.

References

Abdel-Kareem, O., Abdel-Rahim, H., Ezzat, I., & Essa, D. M. (2015). Evaluating the use of chitosan coated Ag nano-SeO2 composite in consolidation of Funeral Shroud from the Egyptian Museum of Cairo. *Journal of Cultural Heritage, 16*(4), 486–495. https://doi.org/10.1016/j.culher.2014.09.016

Ai, Y., Zhang, L., Cui, M., Huang, R., Qi, W., He, Z., et al. (2022). Toward cleaner production of nanocellulose: A review and evaluation. *Green Chemistry, 24*(17), 6406–6434. https://doi.org/10.1039/D2GC01669A

Baglioni, P., & Chelazzi, D. (2021). How science can contribute to the remedial conservation of cultural heritage. *Chemistry – A European Journal, 27*(42), 10798–10806. https://doi.org/10.1002/chem.202100675

Barhoum, A., Deshmukh, K., García-Betancourt, M.-L., Alibakhshi, S., Mousavi, S. M., Meftahi, A., et al. (2023). Nanocelluloses as sustainable membrane materials for separation and filtration technologies: Principles, opportunities, and challenges. *Carbohydrate Polymers, 317*, Article 121057. https://doi.org/10.1016/j.carbpol.2023.121057

Bertolino, V., Cavallaro, G., Lazzara, G., Merli, M., Milioto, S., Parisi, F., et al. (2016). Effect of the biopolymer charge and the nanoclay morphology on nanocomposite

materials. *Industrial & Engineering Chemistry Research, 55*(27). https://doi.org/10.1021/acs.iecr.6b01816. Article 27.
Bertolino, V., Cavallaro, G., Lazzara, G., Milioto, S., & Parisi, F. (2017). Biopolymer-targeted adsorption onto halloysite nanotubes in aqueous media. *Langmuir : the ACS journal of surfaces and colloids, 33*(13). https://doi.org/10.1021/acs.langmuir.7b00600. Article 13.
Bertolino, V., Cavallaro, G., Lazzara, G., Milioto, S., & Parisi, F. (2018). Halloysite nanotubes sandwiched between chitosan layers: Novel bionanocomposites with multilayer structures. *New Journal of Chemistry, 42*(11). https://doi.org/10.1039/C8NJ01161C. Article 11.
Bisht, M., Thayallath, S. K., Bharadwaj, P., Franklin, G., & Mondal, D. (2023). Biomass-derived functional materials as carriers for enzymes: Towards sustainable and robust biocatalysts. *Green Chemistry, 25*(12), 4591–4624. https://doi.org/10.1039/D2GC04792F
Carvalho, D. N., Gonçalves, C., Oliveira, J. M., Williams, D. S., Mearns-Spragg, A., Reis, R. L., et al. (2021). Innovative methodology for marine collagen–chitosan–fucoidan hydrogels production, tailoring rheological properties towards biomedical application. *Green Chemistry, 23*(18), 7016–7029. https://doi.org/10.1039/D1GC02223G
Cavallaro, G., Caruso, M. R., Milioto, S., Fakhrullin, R., & Lazzara, G. (2022). Keratin/alginate hybrid hydrogels filled with halloysite clay nanotubes for protective treatment of human hair. *International Journal of Biological Macromolecules, 222*, 228–238. https://doi.org/10.1016/j.ijbiomac.2022.09.170
Cavallaro, G., Lazzara, G., & Milioto, S. (2012). Aqueous phase/nanoparticles interface: Hydroxypropyl cellulose adsorption and desorption triggered by temperature and inorganic salts. *Soft matter, 8*(13). https://doi.org/10.1039/C2SM07021A. Article 13.
Cavallaro, G., Lazzara, G., Milioto, S., & Parisi, F. (2016). Halloysite nanotubes with fluorinated cavity: An innovative consolidant for paper treatment. *Clay Minerals, 51*(3). https://doi.org/10.1180/claymin.2016.051.3.01. Article 3.
Cavallaro, G., Lazzara, G., Milioto, S., & Parisi, F. (2018). Halloysite nanotubes for cleaning, consolidation and protection. *The Chemical Record, 18*(7–8). https://doi.org/10.1002/tcr.201700099. Article 7–8.
Cavallaro, G., Micciulla, S., Chiappisi, L., & Lazzara, G. (2021). Chitosan-based smart hybrid materials: A physico-chemical perspective. *Journal of Materials Chemistry B, 9*(3), 594–611. https://doi.org/10.1039/D0TB01865A
Cavallaro, G., Milioto, S., Nigamatzyanova, L., Akhatova, F., Fakhrullin, R., & Lazzara, G. (2019). Pickering emulsion gels based on halloysite nanotubes and ionic biopolymers: Properties and cleaning action on marble surface. *ACS Applied Nano Materials, 2*(5), 3169–3176. https://doi.org/10.1021/acsanm.9b00487
Charreau, H., Cavallo, E., & Foresti, M. L. (2020). Patents involving nanocellulose: Analysis of their evolution since 2010. *Carbohydrate Polymers, 237*, Article 116039. https://doi.org/10.1016/j.carbpol.2020.116039
Chen, R., Luo, Z., Yu, X., Tang, H., Zhou, Y., & Zhou, H. (2020). Synthesis of chitosan-based flame retardant and its fire resistance in epoxy resin. *Carbohydrate Polymers, 245*, Article 116530. https://doi.org/10.1016/j.carbpol.2020.116530
Durand-Gasselin, C., Koerin, R., Rieger, J., Lequeux, N., & Sanson, N. (2014). Colloidal stability of zwitterionic polymer-grafted gold nanoparticles in water. *Journal of Colloid and Interface Science, 434*, 188–194. https://doi.org/10.1016/j.jcis.2014.07.048
Egil, A. C., Ozdemir, B., Gunduz, S. K., Altıkatoglu-Yapaoz, M., Budama-Kilinc, Y., & Mostafavi, E. (2022). Chitosan/calcium nanoparticles as advanced antimicrobial coating for paper documents. *International Journal of Biological Macromolecules, 215*, 521–530. https://doi.org/10.1016/j.ijbiomac.2022.06.142
Elmetwaly, T. E., Darwish, S. S., Attia, N. F., Hassan, R. R. A., El Ebissy, A. A., Eltaweil, A. S., et al. (2022). Cellulose nanocrystals and its hybrid composite with inorganic nanotubes as green tool for historical paper conservation. *Progress in Organic Coatings, 168*, Article 106890. https://doi.org/10.1016/j.porgcoat.2022.106890
Faiz Norrrahim, M. N., Mohd Kasim, N. A., Knight, V. F., Mohamad Misenan, M. S., Janudin, N., Ahmad Shah, N. A., et al. (2021). Nanocellulose: A bioadsorbent for chemical contaminant remediation. *RSC Advances, 11*(13), 7347–7368. https://doi.org/10.1039/D0RA08005E
Fang, Y., Chen, L., Wu, J., & Liu, X. (2022). Fire-resistant and antibacterial Chinese Xuan paper by fully bio-based chitosan/phytic acid coating on pulp fibers. *Industrial Crops and Products, 187*, Article 115456. https://doi.org/10.1016/j.indcrop.2022.115456
Farrokhi, Z., Sadjadi, S., Raouf, F., & Bahri-Laleh, N. (2022). Novel bio-based Pd/chitosan-perlite composite bead as an efficient catalyst for rapid decolorization of azo dye. *Inorganic Chemistry Communications, 143*, Article 109734. https://doi.org/10.1016/j.inoche.2022.109734
Gopiraman, M., Deng, D., Saravanamoorthy, S., Chung, I.-M., & Kim, I. S. (2018). Gold, silver and nickel nanoparticle anchored cellulose nanofiber composites as highly active catalysts for the rapid and selective reduction of nitrophenols in water. *RSC Advances, 8*(6), 3014–3023. https://doi.org/10.1039/C7RA10489H
Hu, D., Liu, H., Ding, Y., & Ma, W. (2021). Synergetic integration of thermal conductivity and flame resistance in nacre-like nanocellulose composites. *Carbohydrate Polymers, 264*, Article 118058. https://doi.org/10.1016/j.carbpol.2021.118058
Janakiram, S., Ansaloni, L., Jin, S.-A., Yu, X., Dai, Z., Spontak, R. J., et al. (2020). Humidity-responsive molecular gate-opening mechanism for gas separation in ultraselective nanocellulose/IL hybrid membranes. *Green Chemistry, 22*(11), 3546–3557. https://doi.org/10.1039/D0GC00544D
Kundu, C. K., Hossen, Md. T., Islam, T., Mollick, S., Song, L., & Hu, Y. (2022). Flame retardant coatings from bio-derived chitosan, sodium alginate, and metal salts for polyamide 66 textiles. *ACS Omega, 7*(35), 30841–30848. https://doi.org/10.1021/acsomega.2c02466
Lazzara, G., Parisi, F., Milioto, S., & Haruo, K. (2018). A composition comprising a cellulose nanofiber and halloysite nanotube, a film, and a composite comprising the same (Patent JP2019094482A).
Li, R., Zhang, Y., Lin, Z., Lei, Q., Liu, Y., Li, X., et al. (2021). Injectable halloysite-g-chitosan hydrogels as drug carriers to inhibit breast cancer recurrence. *Composites Part B: Engineering, 221*, Article 109031. https://doi.org/10.1016/j.compositesb.2021.109031
Lin, X., Feng, Y., He, Y., Ding, S., & Liu, M. (2023). Engineering design of asymmetric halloysite/chitosan/collagen sponge with hydrophobic coating for high-performance hemostasis dressing. *International Journal of Biological Macromolecules, 237*, Article 124148. https://doi.org/10.1016/j.ijbiomac.2023.124148
Lisuzzo, L., Cavallaro, G., Milioto, S., & Lazzara, G. (2021). Halloysite nanotubes filled with MgO for paper reinforcement and deacidification. *Applied Clay Science, 213*, Article 106231. https://doi.org/10.1016/j.clay.2021.106231
Lisuzzo, L., Wicklein, B., Lo Dico, G., Lazzara, G., del Real, G., Aranda, P., et al. (2020). Functional biohybrid materials based on halloysite, sepiolite and cellulose nanofibers for health applications. *Dalton Transactions, 49*(12). https://doi.org/10.1039/C9DT03804C. Article 12.
Lombardo, S., & Thielemans, W. (2019). Thermodynamics of adsorption on nanocellulose surfaces. *Cellulose (London, England), 26*(1), 249–279. https://doi.org/10.1007/s10570-018-02239-2
Lu, X., Jiao, H., Shi, Y., Li, Y., Zhang, H., Fu, Y., et al. (2023). Fabrication of bio-inspired anisotropic structures from biopolymers for biomedical applications: A review. *Carbohydrate Polymers, 308*, Article 120669. https://doi.org/10.1016/j.carbpol.2023.120669
Martins, N. C. T., Fateixa, S., & Trindade, T. (2023). Chitosan coated papers as sustainable platforms for the development of surface-enhanced Raman scattering hydrophobic substrates. *Journal of Molecular Liquids, 375*, Article 121388. https://doi.org/10.1016/j.molliq.2023.121388
Mokhena, T. C., & John, M. J. (2020). Cellulose nanomaterials: New generation materials for solving global issues. *Cellulose (London, England), 27*(3), 1149–1194. https://doi.org/10.1007/s10570-019-02889-w
Monfared, M., Mawad, D., Rnjak-Kovacina, J., & Stenzel, M. H. (2021). 3D bioprinting of dual-crosslinked nanocellulose hydrogels for tissue engineering applications. *Journal of Materials Chemistry B, 9*(31), 6163–6175. https://doi.org/10.1039/D1TB00624J
Naumenko, E. A., Guryanov, I. D., Yendluri, R., Lvov, Y. M., & Fakhrullin, R. F. (2016). Clay nanotube–biopolymer composite scaffolds for tissue engineering. *Nanoscale, 8*(13), 7257–7271. https://doi.org/10.1039/C6NR00641H
Naumenko, E., & Fakhrullin, R. (2019). Halloysite nanoclay/biopolymers composite materials in tissue engineering. *Biotechnology Journal, 14*(12). https://doi.org/10.1002/biot.201900055. Article 12.
Ong, X.-R., Chen, A. X., Li, N., Yang, Y. Y., & Luo, H.-K. (2023). Nanocellulose: Recent advances toward biomedical applications. *Small Science, 3*(2), Article 2200076. https://doi.org/10.1002/smsc.202200076
Operamolla, A., Mazzuca, C., Capodieci, L., Di Benedetto, F., Severini, L., Titubante, M., et al. (2021). Toward a reversible consolidation of paper materials using cellulose nanocrystals. *ACS Applied Materials & Interfaces, 13*(37), 44972–44982. https://doi.org/10.1021/acsami.1c15330
Paul, J., & Ahankari, S. S. (2023). Nanocellulose-based aerogels for water purification: A review. *Carbohydrate Polymers, 309*, Article 120677. https://doi.org/10.1016/j.carbpol.2023.120677
Pötzinger, Y., Rahnfeld, L., Kralisch, D., & Fischer, D. (2019). Immobilization of plasmids in bacterial nanocellulose as gene activated matrix. *Carbohydrate Polymers, 209*, 62–73. https://doi.org/10.1016/j.carbpol.2019.01.009
Qu, R., Wang, Y., Li, D., & Wang, L. (2021). The study of rheological properties and microstructure of carboxylated nanocellulose as influenced by level of carboxylation. *Food Hydrocolloids, 121*, Article 106985. https://doi.org/10.1016/j.foodhyd.2021.106985
Rissanen, V., Vajravel, S., Kosourov, S., Arola, S., Kontturi, E., Allahverdiyeva, Y., et al. (2021). Nanocellulose-based mechanically stable immobilization matrix for enhanced ethylene production: A framework for photosynthetic solid-state cell factories. *Green Chemistry, 23*(10), 3715–3724. https://doi.org/10.1039/D1GC00502B
Sadjadi, S., Abedian-Dehaghani, N., Heydari, A., & Heravi, M. M. (2023). Chitosan bead containing metal–organic framework encapsulated heteropolyacid as an efficient catalyst for cascade condensation reaction. *Scientific Reports, 13*(1), 2797. https://doi.org/10.1038/s41598-023-29548-2
Salas, C., Nypelö, T., Rodriguez-Abreu, C., Carrillo, C., & Rojas, O. J. (2014). Nanocellulose properties and applications in colloids and interfaces. *Current Opinion in Colloid & Interface Science, 19*(5), 383–396. https://doi.org/10.1016/j.cocis.2014.10.003
Shi, Y., Jiao, H., Sun, J., Lu, X., Yu, S., Cheng, L., et al. (2022). Functionalization of nanocellulose applied with biological molecules for biomedical application: A review. *Carbohydrate Polymers, 285*, Article 119208. https://doi.org/10.1016/j.carbpol.2022.119208
Spagnuolo, L., D'Orsi, R., & Operamolla, A (2022). Nanocellulose for paper and textile coating: The importance of surface chemistry. *ChemPlusChem, 87*(8), Article e202200204. https://doi.org/10.1002/cplu.202200204
Tamaddon, F., Arab, D., & Ahmadi-AhmadAbadi, E. (2020). Urease immobilization on magnetic micro/nano-cellulose dialdehydes: Urease inhibitory of Biginelli product in Hantzsch reaction by urea. *Carbohydrate Polymers, 229*, Article 115471. https://doi.org/10.1016/j.carbpol.2019.115471
Thakur, V., Guleria, A., Kumar, S., Sharma, S., & Singh, K. (2021). Recent advances in nanocellulose processing, functionalization and applications: A review. *Materials Advances, 2*(6), 1872–1895. https://doi.org/10.1039/D1MA00049G

Vadodaria, S. S., Onyianta, A. J., & Sun, D. (2018). High-shear rate rheometry of micro-nanofibrillated cellulose (CMF/CNF) suspensions using rotational rheometer. *Cellulose (London, England), 25*(10), 5535–5552. https://doi.org/10.1007/s10570-018-1963-4

Wu, T., Kummer, N., France, K. J. D., Campioni, S., Zeng, Z., Siqueira, G., et al. (2021). Nanocellulose-lysozyme colloidal gels via electrostatic complexation. *Carbohydrate Polymers, 251*, Article 117021. https://doi.org/10.1016/j.carbpol.2020.117021

Zhang, X., Morits, M., Jonkergouw, C., Ora, A., Valle-Delgado, J. J., Farooq, M., et al. (2020). Three-dimensional printed cell culture model based on spherical colloidal lignin particles and cellulose nanofibril-alginate hydrogel. *Biomacromolecules, 21*(5), 1875–1885. https://doi.org/10.1021/acs.biomac.9b01745

Zhao, K., Wang, W., Teng, A., Zhang, K., Ma, Y., Duan, S., et al. (2020). Using cellulose nanofibers to reinforce polysaccharide films: Blending vs layer-by-layer casting. *Carbohydrate Polymers, 227*, Article 115264. https://doi.org/10.1016/j.carbpol.2019.115264

Zheng, J., Wu, F., Li, H., & Liu, M. (2019). Preparation of bioactive hydroxyapatite@halloysite and its effect on MC3T3-E1 osteogenic differentiation of chitosan film. *Materials Science and Engineering: C, 105*, Article 110072. https://doi.org/10.1016/j.msec.2019.110072